DYNAMIC MODELING OF THE HEAT TRANSFER PROCESS IN ROTARY KILNS WITH INDIRECT OIL HEATING
Parametric Analysis of Gypsum Calcination Case

by

Jose Junio URBANO[a,b], Jorge Recarte HENRIQUEZ[a], Alvaro Antonio Villa OCHOA[a,b*], Ana Rosa PRIMO[b], and Anderson Breno SOUZA[b,c]

[a] Federal Institute of Technology of Pernambuco, Pernambuco, Brasil
[b] Federal University of Pernambuco, Pernambuco, Brasil
[c] Federal University of Oeste da Bahia, Bahia, Brasil

Original scientific paper
https://doi.org/10.2298/TSCI210523245U

This work proposes a mathematical modeling and numerical simulation of a gypsum rotary kiln with indirect oil heating in a 3-D transient regime. The mathematical model was based on Fourier's law as a constitutive relationship and the principle of energy conservation, applied to a control volume in cylindrical coordinates. Furthermore, a bed homogenization model was used to represent the most realistic condition of the physical phenomenon since some rotary kilns have internal fins that aim at homogenizing the gypsum temperature during calcination. This work intends to fill the gap found in heat transfer processes on rotary kilns in transient regime considering 3-D positions, to have an accurate projection of the temperature profile of the kiln and also, given by the numerical model, the possibility of a tool that can be used to the optimization of the control system of rotary kilns considering the actual demand of the material in production, leading to the best energy performance of the equipment's activation source, as well as reaching the temperatures and processing time of the product. The numerical simulation results revealed reasonable agreement with the experimentally determined calcination process in rotary kilns. Furthermore, a parametric analysis of the influence of the mixture on the temperature fields and the calcination time was carried out to verify the energetic balance of the rotary kiln.

Key words: *dynamic analysis, 3-D simulation, calcination, oil heating system*

Introduction

Gypsum is obtained from the chemical dehydration process of gypsum, which occurs between 80 °C and 160 °C, called calcination, and, usually, for this purpose, it uses rotary kilns [1]. Preferably, when fuels are used that, when burned, generate particulates, they use indirect burning furnaces. This is what happens in the Araripe region in Pernambuco, a significant plaster producer in Brazil, where firewood, fuel oil, and petroleum coke contribute to the predominance of rotary use kilns with indirect burning [2]. In the gypsum calcination process, a considerable amount of CO_2 is emitted, which, together with the emission from the burning of fuels, are relevant sources of pollution and make it necessary to maximize the kilns' effi-

* Corresponding author, e-mail: ochoaalvaro@recife.ifpe.edu.br

ciency obtaining the plaster [3]. The inefficient control of parameters such as the rotation of the furnace and the combustion gases' temperature can result in an inefficient process with excessive energy consumption and forming an inhomogeneous temperature gradient in the obtained plaster. Therefore, the improvement in the heat transfer process in rotary kilns is essential to increase the efficiency and quality of the final product.

In the literature, it is common to find experimental and numerical studies involving heat transfer analysis in different types of furnaces. For example, heat transfer by radiation was evaluated in tasks such as those developed by Opitz *et al.* [4] and Wang and Zhang [5]. In addition, Obando *et al.* [6] analyzed an indirect burning furnace characterized by the predominance of natural convection, while Razazadeh *et al.* [7] studied a direct-burning furnace, where forced convection predominates.

In many studies, they used numerical computer simulations, which can reduce costs and time to execute engineering projects [8]. Approaching the analysis of the calcination process in rotary kilns, the literature reports many works related to the formation of cement [9], including those related to energy recovery and increased system efficiency [10] and almost nothing when the objective is to obtain plaster, where studies concentrate on its basic thermochemical aspects [11], on the dynamics of operation control [12] and exergoeconomic analysis of the kilns [13].

It should be noted that the existing studies, even in different application areas, provide technical subsidies and also essential data that can be applied to the plaster calcination process, which is the main focus of this article. In general, heat transfer in rotary kilns was studied with a view to better uniformity in the temperature of the kiln housing [14], better chemical transformation process in plasterboard [1], optimized development of performance control [15], evaluation profiles of internal and external temperatures in steady-state [16] and simplified analysis of operations in transient regimes [17]. Therefore, this work intends to fill the absence of studies involved in the heat transfer processes in rotary kilns for calcining plaster in a transient regime, considering all three spatial positions, to have a real projection of the oven temperature profile, also contributing to its dimensioning and control process regarding the use of the conditions of non-homogenization and homogenization of the bed in the production of calcination plaster.

Thus, the objective of this work is to develop a mathematical model and perform the numerical simulation of a new calcination system for plaster formation based on indirect heating by the circulation of thermal oil in the walls of the rotary kiln to predict its temperature gradients, the heating rate, the influence of the rotation, temperature and mass flow of the system oil and homogenization of its bed.

Mathematical modeling

In this section, the physical problem (rotary kiln) description will be presented, involving the kiln operation's main characteristics and geometry.

Description of the physical problem – rotary furnace

The rotary kiln for gypsum calcination, used for analysis in the present work, is of indirect heating and consists of two concentric cylinders, with the external cylinder fixed and the internal one moving with a low rotation speed (up to 4 rpm) about the external cylinder during the calcination operation. The bed of gypsum particles, which is deposited in the inner cylinder, moves according to rotation speed with a movement configuration that depends on the speed of rotation and other construction factors that promote the homogenization of the bed temperature. Figure 1 shows a diagram of the cross-section of the calcination furnace.

The calcination process analyzed with this furnace takes place in batch so that the load heats up in a dynamic process until it reaches the calcination temperature. This condition indicates the end of the process.

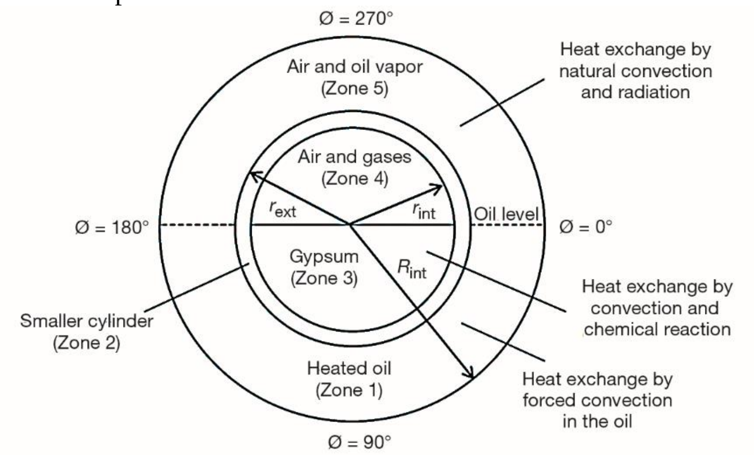

Figure 1. Schematic representation of a cross-section of the rotary furnace

Mathematical model of a rotary furnace

The mathematical model of the furnace, according to with a description of section *Description of the physical problem – rotary furnace* and fig. 1, was built considering a physical domain segmented into five zones: zone composed by the heated oil, zone formed by the smaller cylinder with low rotation speed, zone formed by the gypsum bed, zone formed by the volume above the gypsum bed, composed of air and gases from the calcination process, and zone formed by the volume above the heated oil in the region of the concentric cylinders, composed of air and oil vapors.

Zone 1. Heated oil

Zone 1 is formed by the heating oil, which flows in the lower half of the annular space between the concentric cylinders in the axial direction of the furnace, z. Applying an energy balance to this region, considering a differential segment in the flow direction (axial direction), eq. (1) is obtained, valid for $0 \leq Ø \leq 180°$, $0 \leq z \leq L$, and $r_{ext} \leq r \leq r_{int}$. The angular direction is being measured counterclockwise. In this energy balance, it was considered that the external wall of the furnace is perfectly insulated.

$$m_{oil} c_p \frac{\partial T_{oil}}{\partial t} = (\dot{m}_{in} c_p T_{in_{oil}} - \dot{m}_{out} c_p T_{out_{oil}}) + hA(T_{cyl} - T_{oil}) \tag{1}$$

The correlation used to calculate the convection heat transfer coefficient is given by:

$$\mathrm{Nu}_{oil} = \frac{\bar{h} D_h}{k_{oil}} = 0.0296 \,\mathrm{Re}^{4/5} \,\mathrm{Pr}^{1/3} \tag{2}$$

This correlation corresponds to the flow over an isothermal plate and is valid $\mathrm{Re} \leq 10^8$ and $0.6 \leq \mathrm{Pr} \leq 60$.

Zone 2. Internal cylinder

Applying the energy balance in a differential element of the domain zone, Zone 2 is formed by the internal steel cylinder, for $0 \leq Ø \leq 360°$, $0 \leq z \leq L$, and $r_{int} \leq r \leq r_{ext}$:

$$\frac{1}{r}\frac{\partial}{\partial r}\left(k_{cyl} r \frac{\partial T_{cyl}}{\partial r}\right)+\frac{1}{r^2}\frac{\partial}{\partial \varnothing}\left(k_{cyl}\frac{\partial T_{cyl}}{\partial \varnothing}\right)+\frac{\partial}{\partial z}k_{cyl}\left(\frac{\partial T_{cyl}}{\partial z}\right)=\rho_{cyl}c_{p,cyl}\frac{\partial T_{cyl}}{\partial t} \tag{3}$$

For this equation, the boundary conditions are specified from the interrelation that Zone 2 has with the other domains of the problem. Inside $r = r_{int}$ $180 \leq Ø \leq 360°$, and $0 \leq z \leq L$ there is a heat transfer by convection with the gas mixture formed by air and gases from calcination and heat transfer by thermal radiation with the free surface of the gypsum:

$$k_{cyl}\left.\frac{\partial T_{cyl}}{\partial r}\right|_{r_{int}}=q_{rad}+q_{conv} \tag{4}$$

The radiation is treated as a cavity with two surfaces, and the resulting equation is given by eq. (5). In turn, the convection is determined based on Newton's cooling law, and the convective coefficient is defined by eq. (6).

$$q_{rad}=\frac{\sigma(T_{cyl}^4-T_{gyp}^4)}{\dfrac{1-\varepsilon_{gyp}}{\varepsilon_{gyp}A_{gyp}}+\dfrac{1}{A_{gyp}F_{cyl,gyp}}+\dfrac{1-\varepsilon_{cyl}}{\varepsilon_{cyl}A_{cyl}}} \tag{5}$$

$$h_{air,cyl,int}=0.46\frac{k_g}{D_e}\text{Re}_D^{0.535}\text{Re}_\omega^{0.104}\eta^{-0.341} \tag{6}$$

where k_g is the thermal conductivity of the gas, D_e – the hydraulic diameter, Re_D and Re_ω – the axial and angular Reynolds numbers, respectively, and η – the bed filling factor. The angle θ indicates the height of the bed in the cylinder and defines the parameters hydraulic diameter and fill factor. In the specific case of this study, the value of θ is equal to π, and therefore the filling factor will be equal to 0.5, indicating that the bed occupies half the cylinder:

$$\text{Re}_D=\frac{u_g D_e}{\nu_g} \tag{7}$$

$$\text{Re}_\omega=\frac{\omega D_e^2}{\nu_g} \tag{8}$$

$$\eta=\frac{2\theta-\sin(2\theta)}{2\pi} \tag{9}$$

$$D_e=\frac{0.5D[2\pi-2\theta+\sin(2\theta)]}{[\pi-\theta+\sin\theta]} \tag{10}$$

In $r = r_{ext} 180 \leq Ø360°$ and $0 \leq z \leq L$, Zone 2, heat exchange through convection and thermal radiation, and the boundary condition are defined by eq. (11). These two forms of heat transfer were treated as occurring in a cavity (annular space) formed by concentric cylinders filled with a mixture of air and steam of thermal oil. Convection in this type of problem can be treated through effective thermal conductivity, which assumes that a stationary fluid will transfer the same amount of heat as a real fluid in motion. The correlation for k_{ef} suggested by [17] was used, with F_C being the geometric factor of concentricity of the cylinders expressed by eq. (13).

$$k_{cyl}\left.\frac{\partial T_{cyl}}{\partial r}\right|_{r_{ext}}=q_{rad}+q_{conv} \tag{11}$$

$$\frac{k_{ef}}{k}=0.386\left(\frac{\text{Pr}}{0.861+\text{Pr}}\right)^{1/4}(F_C\,\text{Ra}_c)^{1/4} \tag{12}$$

$$F_C=\frac{\left(\ln\dfrac{D_o}{D_i}\right)^4}{L_C^3\left(D_i^{\frac{-3}{5}}+D_o^{\frac{-3}{5}}\right)^5} \tag{13}$$

$$\text{Ra}_L=\frac{g\beta(T_s-T_{inf})L_C^3}{\nu^3}\text{Pr} \tag{14}$$

Equation (13) is valid for $0.7\leq\text{Pr}\leq6000$ and $10^2\leq F_C\text{Ra}_c\leq10^7$. For $F_C\text{Ra}_c<10^2$ the natural convection current can be neglected and $k_{ef}=k$. The properties of the fluid should be evaluated at the average temperature. Natural convection was admitted in this treatment, considering the low rotation speed of the internal cylinder.

The heat transfer by thermal radiation was determined considering an average cavity formed by concentric cylinders, represented by eq. (15). For simplification, heat transfer in a non-participating medium was considered.

$$q_{rad}=-\frac{\sigma A_1(T_1^4-T_2^4)}{\dfrac{1}{\varepsilon_1}+\dfrac{1-\varepsilon_2}{\varepsilon_2}\left(\dfrac{r_1}{r_2}\right)} \tag{15}$$

In $r=r_{int}$n, $0\leq Ø\leq180°$ and $0\leq z\leq L$ in Zone 2 (bottom of the cylinder), there is a thermal exchange between the surface of the cylinder and the gypsum bed. This heat transfer occurs by thermal contact, so an energy balance by conducting heat at the border will represent the boundary condition according to:

$$k_{cyl}\left.\frac{\partial T_{cyl}}{\partial r}\right|_{r_{int}}=k_{gyp}\left.\frac{\partial T_{gyp}}{\partial r}\right|_{r_{int}} \tag{16}$$

In $r=r_{ext}$ $0\leq Ø\leq180°$ and $0\leq z\leq L$, Zone 2, the convection heat transfer between the thermal oil and the inner cylinder surface is computed through eq. (17). The average convective coefficient is the same as in eq. (1) and obtained by the correlation for Nusselt given by eq. (2).

$$k_{\text{cyl}} \frac{\partial T_{\text{cyl}}}{\partial r}\bigg|_{r_{\text{ext}}} = h(T_{\text{cyl}} - T_{\text{oil}}) \tag{17}$$

Zone 3. Zone formed by the gypsum bed

Equation (18), valid for $0 \le Ø \le 180°$, $0 \le z \le L$, and $0 \le r \le r_{\text{int}}$, allows treating heat transfer by diffusion within the gypsum bed. In this formulation, it is considered that the gypsum occupies the lower half of the inner cylinder.

$$\frac{1}{r}\frac{\partial}{\partial r}\left(k_{\text{gyp}} r \frac{\partial T_{\text{gyp}}}{\partial r}\right) + \frac{1}{r^2}\frac{\partial}{\partial \varnothing}\left(k_{\text{gyp}} \frac{\partial T_{\text{gyp}}}{\partial \varnothing}\right) + \frac{\partial}{\partial z}\left(k_{\text{gyp}} \frac{\partial T_{\text{gyp}}}{\partial z}\right) + \dot{q} = \rho_{\text{gyp}} c_{p,\text{gyp}} \frac{\partial T_{\text{gyp}}}{\partial t} \tag{18}$$

Gypsum is calcium sulfate dehydrate ($CaCO_4 2H_2O$). When it is subjected to a heating process, it loses the chemically trapped water in the crystalline network. This process is known as calcination and is treated in the literature as a two-step process that corresponds to endothermic reactions. The technical [1] reported that the first stage starts at around 80°C and extends to a temperature in the order of 160 °C.

In this work, only the formation of hemihydrate calcium sulfate is of interest; therefore, only the first step is incorporated in the model through the amount of energy consumed in the reaction and quantified in eq. (18) in the internal energy generation term, $\dot{q}$.

The convective coefficient is defined by eq. (18) obtained from [17] subject to the same consideration's parameters defined by fig. 2 and eqs. (7)-(10).

$$h_{\text{air,gyp}} = 0.54 \frac{k_g}{De} \text{Re}_D^{0.575} \text{Re}_\omega^{-0.292} \tag{19}$$

Zone 4. Zone formed by air and gases from the calcination process

The zone formed by air and gases from the calcination process is defined by geometric parameters $180 \le Ø \le 360°$, $0 \le z \le L$, and $0 \le r \le r_{\text{int}}$ eq. (19) is applied by applying an energy balance in this domain that exchanges energy by convection with the inner walls of the inner cylinder and with the free surface of the gypsum. Convective coefficients follow eqs. (6) and (19):

$$m_{\text{air}} c_{p,\text{air}} \frac{\partial T_{\text{air}}}{\partial t} = h_{\text{air,cyl,int}} A(T_{\text{cyl,int}} - T_{\text{air}}) - h_{\text{air,gyp}} A(T_{\text{air}} - T_{\text{gyp}}) \tag{20}$$

Zone 5. The zone formed by air and thermal oil vapor

In this same zone of the domain, there will be heat exchange for radiation (concentric cylinder cavity), according to eq. (14). In this equation r_1 [m] is the radius of the smallest cylinder and r_2 [m] – the radius of the large cylinder. Heat will also be exchanged by natural convection (concentric cylinders) with air and oil vapors. The effective thermal conductivity of a fictitious stationary fluid will transfer the same amount of heat as a real fluid in motion. The suggested correlation for k_{ef}, according to [16] is:

$$\frac{k_{\text{ef}}}{k} = 0.386 \left(\frac{\text{Pr}}{0.861 + \text{Pr}}\right)^{1/4} (F_{\text{C}} \, \text{Ra}_{\text{c}})^{1/4} \tag{21}$$

where Ra_C is the number of Rayleigh given by eq. (14) and F_C – the geometric factor of concentricity of the cylinders given by eq. (13). Although the model is 3-D, the longitudinal temperature field did not show significant variation (less than 1%), making the behavior of the 2-D model.

Calibration and validation of the modeling

This section will present the calibration process according to the mesh independence study and model symmetry tests. Finally, the Validation of the results will be presented through the operational data of a rotary kiln of indirect burning with the results found by the developed numerical model.

For the discretization of the equations, the finite volume method (FVM) was used with explicit formulation for a cylindrical co-ordinate system. The MATLAB® platform was used for the numerical solution of the model's discretized equations. Initially, data on the dimensions of the furnace and the mesh in cylindrical co-ordinates are provided, together with the initial temperatures of the oil, gypsum, and air. Next, thermal properties are provided, and the Biot and Fourier number dimensionless parameters are calculated with these and the convection heat transfer coefficients.

To satisfy the stability criterion required in the explicit formulation of the FVM, it was necessary to find the parameters for which this criterion is satisfied. Since these coefficients have a relationship involving the values of the size of the spatial mesh, Δr, $\Delta\emptyset$, Δz, and the temporal mesh, Δt, the maximum time interval was determined Δt given predefined spatial mesh size.

Mesh independence

By analyzing the results in fig. 2(a), it can be seen that the mesh from 80 radial divisions presents a temperature profile practically unchanged (variation of 3% about the 90 radial divisions mesh). In this way, all simulations were performed using a mesh with 100 radial divisions.

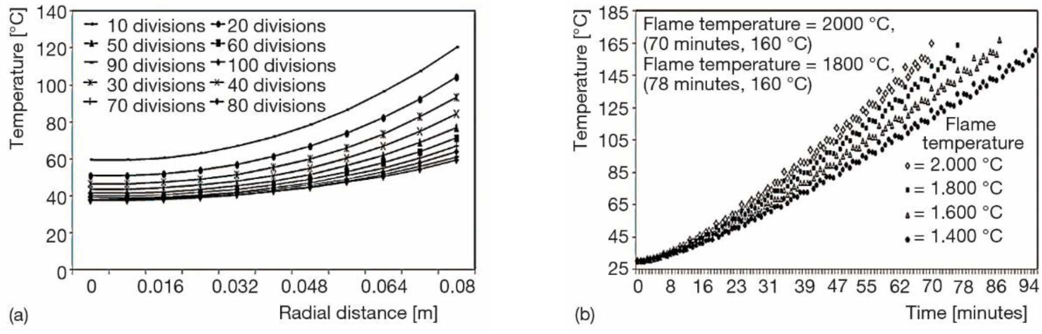

Figure 2. (a) Temperature profiles of a superficial cross-section of the furnace: mesh refining in the radial co-ordinate and (b) heating curve for different burner flame temperatures

All tests used the same time step, Δt = 0.2379 seconds, and the same number of steps in time, 10000 steps in time. The choice of Δt = 0.2379 seconds was made according to the shortest time interval calculated by the temporal stability criterion of the analyzed meshes. In this way, the stability criterion is assured, and the results for each radial mesh size can be compared under the same time-step conditions.

Model independence

The validation of the mathematical model of the oil heating system was carried out by selecting real gypsum calcination conditions such as gypsum mass (by batch), geometrical dimensions of the rotary kiln, and flame temperatures of the burners of an indirect rotary kiln found in the Araripe region. The gypsum mass, which is calcined by batch, is 15000 kg, and its residence time is controlled by monitoring the temperature of the mass contained within the furnace. Upon reaching 160 °C, the furnace is discharged and fed again for the next batch. The batch calcination time is approximately 60 minutes (data provided by the calcining company responsible for the furnace).

Figure 2(b) shows four gypsum heating curves for four different flame temperatures, 1400 °C, 1600 °C, 1800 °C, and 2000 °C, and their respective calcination times.

In computer simulation, the oil temperature is equal to the flame temperature. For the real flame temperature of 2000 °C, the calcination time was approximately 70 minutes, showing a reasonable approximation to the real conditions (60 minutes). For the flame temperature of 1800 °C, the calcination time was around 78 minutes. As expected, increasing the flame temperature reduces the calcination time.

Results and discussion

In this section, a parametric study of the numerical model developed for the simulation of rotary kilns with indirect firing will be presented through two operating conditions: A rotary furnace without mixing and a rotary furnace.

Rotary furnace without homogenization

In this first simulation, it was assumed that the gypsum has a sliding movement about the wall of the rotary kiln, so the mixing of the same over the rotary kiln occurs very slowly. This sliding phenomenon occurs at low speeds and directly relates to Froude's rotational number [18].

It is noted that the points located near the furnace wall have higher temperatures and their rates of temperature increase were also higher since they are closer to the heat source. The heat transfer rate by conduction inside the gypsum was slow due to its low thermal conductivity.

Figure 3(a) shows the heating curve as a function of time for the central point for three different rotations of the furnace: 1 rpm, 4 rpm, and 10 rpm.

It is noticed that there is practically no influence of the rotation on the heating rate, considering each of the three rotations and 500 °C for oil inlet temperature and a mass flow of 30 kg/s. Figure 3(b) shows the influence of the mass oil flow on the heating curve.

This graph shows the temperature evolution, to time, to the point closest to the wall that reached the final calcination temperature. Note that for the mass flow rate of 30 kg/s, the calcination time of the point most relative to the kiln wall was approximately 70 minutes, on the other hand, for the lowest mass flow rate, 10 kg/s, the calcination time is relatively high (430 minutes or 7.2 hours). This is related to the heat exchange by forced convection of the oil with the furnace wall, increasing as the mass flow increases.

Figure 4(a) shows the temperature profiles for three different rotations and a residence time of 3 hours.

By analyzing the initial results, it is possible to verify the thermal infeasibility of this heating process due to the high temperature gradient existing throughout the furnace. The chemical transformation of gypsum into a plaster is not uniform throughout the kiln.

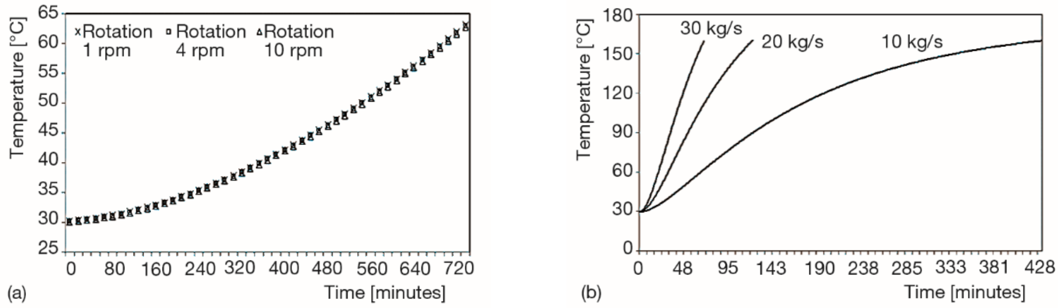

Figure 3. (a) Central point heating curves for three different rotations for a residence time of 3 hours, and (b) influence of the mass-flow of oil on the heating curve to the point close to the wall

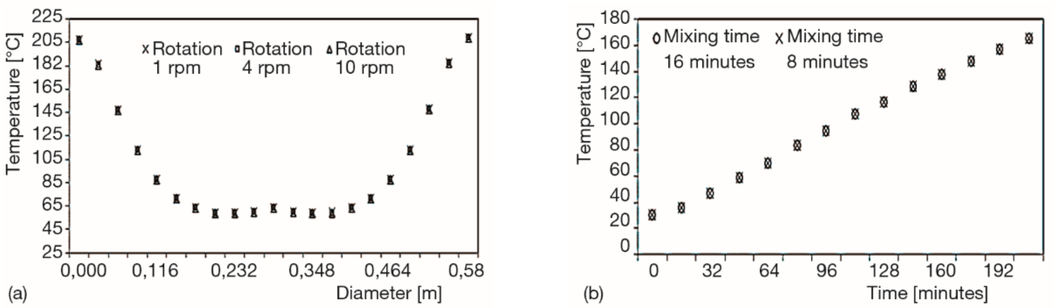

Figure 4. (a) Temperature profiles for three different speeds for a residence time of 3 hours and (b) gypsum temperature for two different mixing times: 8 and 16 minutes

This is a severe problem, as already discussed. Above 160 °C, the gypsum starts to be transformed into active anhydrite, $CaSO_4$. Active anhydrite is unstable and very eager for water and has different physical and mechanical characteristics from plaster. In addition, a long residence time of the material would be necessary for the central point to reach the final calcination temperature, making the process, from a productive point of view, also unfeasible.

Rotary furnace with homogenization

In this simulation, after mixing the gypsum inside the furnace, the temperature was considered to be the weighted average of the temperature of each control volume, according to:

$$T_{\text{ave}} = \frac{\sum_{i=1}^{N} m_i T_i}{\sum_{i=1}^{N} m_i} \tag{21}$$

According to [18], a bed is a critical time to suffer a perfect mixture. The critical time in which the mixture can be considered excellent is given by:

$$t_R = N_{\text{mix}} t_{\text{mix}} \tag{22}$$

The term N_{mix} represents the mixing coefficient and is given by $N_{\text{mix}} = C\text{Fr}^x$, where for rotating equipment $C = 16$ and $x = 0.20$. The Fr is the Froude rotational number given by

Fr = $\omega^2 R$/g, where ω [radians/s] is the rotation speed of the furnace and R [m] – the cylinder's internal radius.

The term $t_{\rm mix}$ represents the time required for a complete revolution of the rotary kiln. After perfect mixing of the gypsum inside the furnace, the temperature was considered to be the weighted average of the temperature of each control volume given by eq. (22). In fig. 4(b), it can be seen that there is no variation in temperature behavior as a function of time for the two mixing time intervals used t_R and $2t_R$.

Figure 5(a) shows the heating curve of the gypsum, as a function of time, for furnace rotations of 1 rpm, 2 rpm, 4 rpm, and 10 rpm with oil inlet temperature and oil mass flow of 500 °C and 20 kg/s, respectively.

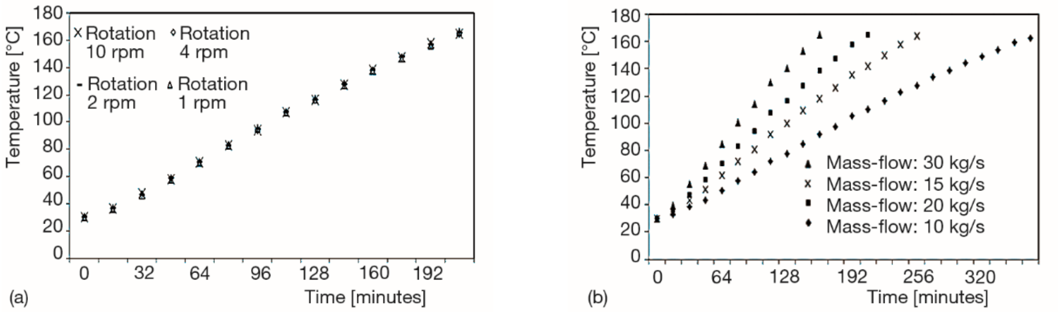

Figure 5. (a) Gypsum temperature for some different speeds and (b) gypsum heating curves for some mass oil flow rates

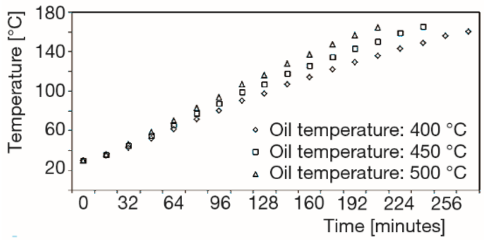

Figure 6. Behavior of the gypsum heating curve as a function of the inlet oil temperature

Figure 5(b) shows the behavior of the gypsum heating curve for some mass oil flow rates. For the mass-flow of 30 kg/s, all the gypsum was calcined in 160 minutes, on the other hand, for the lowest mass-flow, 10 kg/s, all the material was calcined in 368 minutes (6.1 hours). Thus, as the mass-flow rate of oil decreases, the gypsum calcination time increases, and this is related to the heat exchange process by forced oil convection with the furnace wall.

Figure 6 shows the behavior of the heating curve for the oil inlet temperatures of 400, 450, and 500 °C.

For the oil inlet temperature of 400 °C, the calcination time was 272 minutes (4.5 hours), conversely, for the temperature of 500 °C, the calcination time was 208 minutes (3.5 hours). Thus, by increasing the oil inlet temperature, the calcination time is reduced.

Comparison between the operation models with and without homogenization

Figures 7(a) and 7(b) show the two different models for the same operating conditions: oil temperature 500 °C, rotation speed 4 rpm, and mass-flow 30 kg/s. In the model without homogenization, high temperature gradients can be seen, which will result in the non-homogeneous transformation of the gypsum. Furthermore, the first point reaches 160 °C after approximately 70 minutes, while many other issues are at 30 °C. On the other hand, the model with homogenization of all gypsum uniformly reaches the calcination temperature of 160 °C with a residence time of 160 minutes.

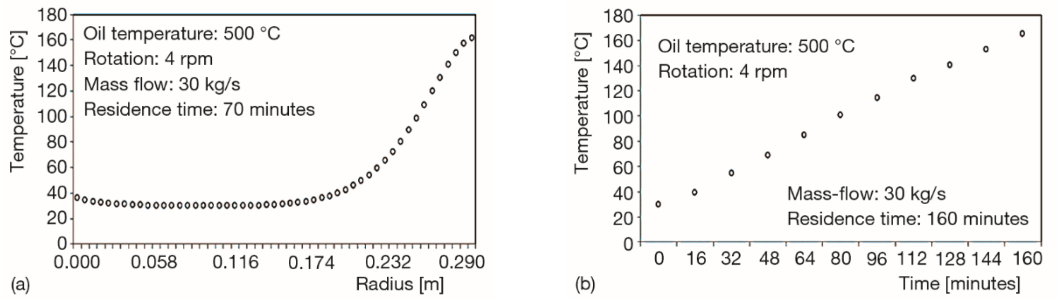

Figure 7. (a) Behavior of the gypsum heating curve in the model without homogenization and (b) behavior of the gypsum heating curve in the model with homogenization

Conclusions

- Considering the rotary kiln model without homogenization of the bed, the thermal infeasibility of this heating process was verified due to the high temperature gradient existing throughout the kiln (figs. 6 and 11): the chemical transformation of gypsum in plaster is not uniform throughout the process. This is a severe problem since between 170 and 250 °C, the calcined gypsum (plaster) becomes active anhydrite ($CaSO_4$).
- Heat rejected by some internal process can be used to heat the oil. Currently, all the heat waste from the gypsum calcination processes is released into the atmosphere. This rejected heat can be used both for heating the oil and for pre-heating the gypsum.
- Satisfactory results were obtained considering the rotary kiln model with homogenization of the bed, related to the calcination time. The entire mass of gypsum calcines evenly, and there is no presence of high-temperature gradients in the gypsum (figs. 7-10 and 12). Therefore, this indicated that the higher the oil temperature at the inlet and the higher the mass flow rate, the shorter the gypsum calcination time will be, regardless of the rotation range.

Acknowledgment

The first author thanks FACEPE for his Doctorate scholarship and the CAPES and PPGEM/UFPE to support the research. The second and third author thanks the CNPq for the scholarship of Productivity.

Nomenclature

A – area, [m^2]
c_p – specific heat, [kJkg^{-1}K^{-1}]
D – diameter [m]
F_C – geometric cylinder concentricity factor, [–]
Gr – Grashof number, $\{=[g\beta(T_s - T_{\text{inf}})L_C^3]/\nu^3\}$, , [–]
h – convection heat transfer coefficient, [Wm^{-2}K^{-1}]
k – coefficient of thermal conductivity, [Wm^{-2}K^{-1}]
m – mass, [kg]
Nu – Nusselt number (= hD/k), [–]
Pr – Prandtl number (= ν/α), [–]
q – rate of heat transfer, [W]
r – radial direction, [m]
Ra$_L$ – Rayleigh number, (= GrPr), [–]
Re – Reynolds number, (= UD/n), [–]
T – temperature, [°C]
t – time, [s]
u_g – average axial transport speed, [ms^{-1}]
z – axial direction, [m]

Greek symbols

Ø – angular direction, [°]

β – coefficient of thermal volumetric expansion, [K^{-1}]
ε – emissivity, [–]
ν – kinematic viscosity, [m^2s^{-1}]
ρ – specific mass, [kgm^{-3}]
σ – Stefan-Boltzmann coefficient [$Wm^{-2}K^{-4}$]
ω – angular speed, [rad s^{-1}]

Subscripts

cond – conduction
conv – convection
cyl – steel cylinder
ext – external
gyp – gypsum
int – internal
rad – radiation

References

[1] John, J., Parametric Studies of Cement Production Processes, *Journal of Energy, 2020* (2020), ID 4289043
[2] Oliveira, M. A. C., Shinohara, A. H., Experience with Natural Gas/LPG in the Plasterer Polo Araripe, PE, Brazil, *Cerâmica, 60* (2014), 354, pp. 243-253
[3] Filkoski, R. V., *et al.*, Energy Optimisation of Vertical Shaft Kiln Operation in the Process of Dolomite Calcination, *Thermal Science, 22* (2018), 5, pp. 2123-2135
[4] Opitz, F., *et al.*, Modeling of Radiative Heat Transfer in an Electric Arc Furnace, *The Minerals, Metals & Materials Society and ASM International, 48B* (2017), Aug., pp. 3301-3315
[5] Wang, Q. M., Zhang, G., Strategy of Thermal Radiation Coatings in Rongdao Kiln of Ceramic Design Industry, *Thermal Science, 23* (2019), 5A, pp. 2793-2800
[6] Obando, J., *et al.*, Theoretical, Experimental and Numerical Study of Infrared Radiation Heat Transfer in a Drying Furnace, *Applied Thermal Engineering, 90* (2015), 3, pp. 395-402
[7] Razazadeh, N., *et al.*, Effect of Burners Configuration on Performance of Heat Treatment Furnaces, *International Journal of Heat and Mass Transfer, 136* (2019), June, pp. 799-807
[8] Wang, H., *et al.*, Heat Transfer Calculation Methods in Three-Dimensional CFD Model for Pulverized Coal-Fired Boilers, *Applied Thermal Engineering, 166* (2020), Feb., 114633
[9] Afkhami, B., *et al.*, Energy Consumption Assessment in a Cement Production Plant, *Sustainable Energy Technologies and Assessments, Sustainable Energy Technologies and Assessments, 10* (2015), June, pp. 84-89
[10] Akram, N., *et al.*, Improved Waste Heat Recovery Through Surface of Kiln Using Phase Change Material, *Thermal Science, 22* (2018), 2, pp. 1089-1098
[11] Bordons, C., Dorado, F., Non-Linear Models for Agypsumkiln, A Comparative Analysis, *Proceedings*, 15th Triennial World Congress, Barcelona, Barcelona, Spain, 2002, Vol. 35, pp. 271-276
[12] Gürtürk, M., Oztop, H. F., Exergoeconomic Analysis of a Rotary Kiln Used for Plaster Production as Building Materials, *Applied Thermal Engineering, 104* (2016), July, pp. 486-496
[13] Herz, F., *et al.*, Influence Of Operational Parameters and Material Properties on the Contact Heat Transfer in Rotary Kilns, *International Journal of Heat and Mass Transfer, 55* (2012), 25-26, pp. 7941-7948
[14] Machalek, D., Powell, K. M., Model Predictive Control of a Rotary Kiln for Fast Electric Demand Response, *Applied Thermal Engineering, 144* (2019), Dec., 106021
[15] Boateng, A. A., Barr, P. V., A Thermal Model for the Rotary Kiln Including Heat Transfer Within the Bed, *International Journal of Heat and Mass Transfer, 39* (1996), 10, pp. 2131-2143
[16] Spiridon, O., *et al.*, Simulation Model for the Transient Process Behaviour of Solar Aluminium Recycling in a Rotary Kiln, *Applied Thermal Engineering, 78* (2015), Mar., pp. 387-396
[17] Raithby, G. D., Hollands, K. G., Laminar and Turbulent Heat Transfer by Natural Convection, *Heat Mass Transfer, 17* (1974), 12, pp. 1620-1622
[18] Devahastin S, Mujumdar A., *Indirect Dryers Third Edition*, Taylor and Francis Group., New York, USA, 2006

Paper submitted: May 23, 2021
Paper revised: June 22, 2021
Paper accepted: June 27, 2021